Eur Spine J (2013) 22 (Suppl 4):S567–S578
DOI 10.1007/s00586-012-2333-9

REVIEW ARTICLE

Imaging findings of Pott's disease

Antonio Rivas-Garcia · Silvana Sarria-Estrada · Carme Torrents-Odin · Lourdes Casas-Gomila · Elisa Franquet

Received: 28 October 2011 / Accepted: 17 April 2012 / Published online: 9 June 2012

Abstract Tuberculosis (TB) continues to be an important public health problem in developed countries especially in deprived socioeconomic groups, older people, immunocompromised patients, drug-therapy resistant cases and the immigrant population. The spine is the most frequent location of musculoskeletal TB. The wide range of clinical presentations results in difficulties and delays in diagnosis. Advanced disease mimics other infections and malignancy. The diagnosis of spinal infections relies on three main factors: clinical symptoms, imaging and bacteriological culture. Advanced imaging such as Magnetic Resonance Imaging (MRI), Multidetector Computed Tomography (MDCT) and Fluor18-Deoxiglucose Positron Emission Tomography combined with CT (F-18 FDG PET–CT) demonstrate lesion extent, serve as guide for biopsy with aspiration for culture, assist surgery planning and contribute to follow-up. Diagnosis of TB cannot be established solely on the basis of clinical tests or imaging findings and biopsy may be required. Differential diagnosis between tuberculous and pyogenic spondylitis is of clinical importance, but may be difficult on the basis of radiological findings alone. Findings not pathognomonic but favoring tuberculous etiology include: slow progression of lesions with late preservation of disk space, involvement of several contiguous segments, large intraosseous and paraspinal abscesses containing calcifications, and body collapse with kyphotic deformity. In this essay the highlights of TB imaging are reviewed through published literature. In addition, we review retrospectively the radiological findings of 48 patients with tuberculous spondylitis treated from 1993 to 2010. There were 23 male and 25 female patients with a mean age of 53 years.

Keywords Tuberculosis · Spinal infection · Imaging modalities · Imaging-guided percutaneous biopsy

A. Rivas-Garcia (✉) · C. Torrents-Odin · L. Casas-Gomila
Department of Radiology, Hospital Vall ′de Trauma Vall d′Hebron, P. Vall d′Hebron 119-129, 08035 Barcelona, Spain
e-mail: 10804arg@comb.es

C. Torrents-Odin
e-mail: ctorrent@vhebron.net

L. Casas-Gomila
e-mail: lcasas@vhebron.net

S. Sarria-Estrada
IDI-RM Unit, Department of Radiology, Hospital Vall d′Hebron, Barcelona, Spain
e-mail: shanasarria@yahoo.com

E. Franquet
Department of Nuclear Medicine, Hospital Vall d′Hebron, Barcelona, Spain
e-mail: eli_franquet@hotmail.com

Introduction

Spinal infections represent 2–4 % of all cases of osteomyelitis and the most common causative organisms are pyogenic, but nonpyogenic bacteria represent a serious disease, which requires early diagnosis and prompt treatment. The latter show a subacute or chronic course and include Brucella, fungi, parasites and especially Mycobacterium tuberculosis (MTB). Also known as "Pott's Disease" tuberculous spondylitis represents the most common form of extrapulmonary TB [1].

Musculoskeletal involvement of TB is estimated in 1–13 % of patients and spine is affected in more than 50 % of cases [2–9]. It is most prevalent in adults with no sex predominance [10–12]. The thoracic segments are the preferred sites in which infection spreads, followed by the

lumbar levels [2–5, 7, 11, 13–18]. The disease often involves two contiguous vertebral bodies with the intervening disk, but multilevel extension (three or more vertebrae) is not uncommon and characterizes the disease. In addition, single or multiple vertebral involvement preserved disk has been recognized [3, 4, 10–13, 19]. It remains unclear whether the multivertebral disease is a consequence of hematogenous dissemination or it is a direct subligamentous, paraspinal or subarachnoid spread disease [20], although subligamentous spread seems most likely [12].

Definitive diagnosis is often difficult because its clinical presentation is indistinct and nonspecific [9, 20, 21]. Longstanding back pain and constitutional symptoms predominate [2]. This results in delayed diagnosis and increased morbidity due to complications such as cold abscesses, sinus tracts, neurological weakness, vertebral collapse and kyphosis [5, 14].

Accurate interpretation of imaging requires experience and understanding of spinal anatomy and pathophysiology. The sources of spinal infection can be hematogenous spread through arterial vessels, postoperative infection, direct puncture or trauma and also spread from a contiguous focus [1, 7, 22]. Spinal spread is thought to be hematogenous in most instances [5, 22]. Anatomic distribution of vertebral vessels is age related. In adults, the richly vascularized vertebral zone is the vertebral body corner adjacent to end plate (spondylitis), and as such is the most common site of initial infection (Fig. 1) [1, 5, 11, 21]. Further the infection spreads within the vertebral body, to the opposite endplate, to the disk space (spondylodiskitis), to the vertebral arch, and beneath the anterior or posterior longitudinal ligaments, leading to extension of the infection to multiple adjacent or separate vertebral segments (Fig. 2) [1, 4, 8, 9, 23].

MTB doesn't produce proteolytic enzymes and this implies relative preservation of disk space [8, 9]. The histological pattern consists of the formation of tubercles with central caseating necrosis giving extensive inflammatory masses (phlegmon) and cold abscesses spreading along bone, disk and soft tissues. In late disease, tubercles are replaced with fibrous tissue and calcification of caseating areas may occur [1]. Progressive necrosis of bone leads to vertebral osteolysis that produces kyphosis and instability. In rare cases the infection affects paraspinal tissues, vertebral body or vertebral arch exclusively (Fig. 3) [1, 19].

The differential diagnosis includes atypical degenerative disk disease, pyogenic and fungal infections, granulomatous diseases as sarcoidosis, deposition diseases, inflammatory and neuropathic spondyloarthropaties and also malignant processes as metastasis or lymphoma [1, 5, 20, 22, 24, 25].

Radiography and CT findings

Although radiographs may be normal in the early stage of disease [1, 19], plain films continue to be the initial screening procedure when infectious spondylitis is suspected

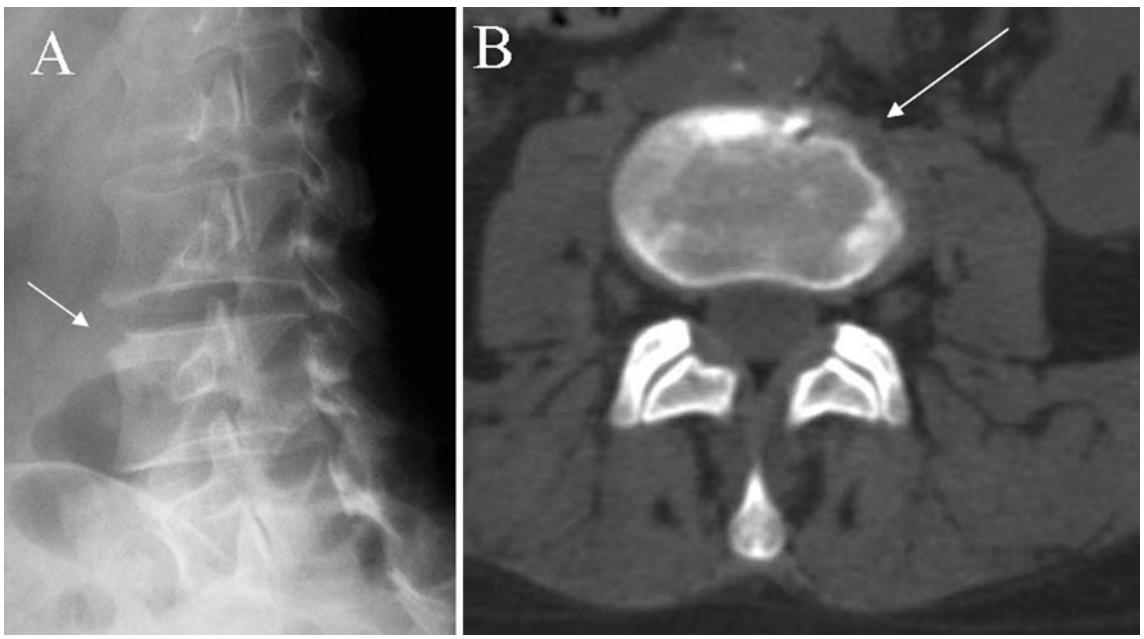

Fig. 1 **a**, **b** X-rays oblique view and axial CT scan show early erosive changes typically located in the anterolateral corner of the vertebral body (*arrows*)

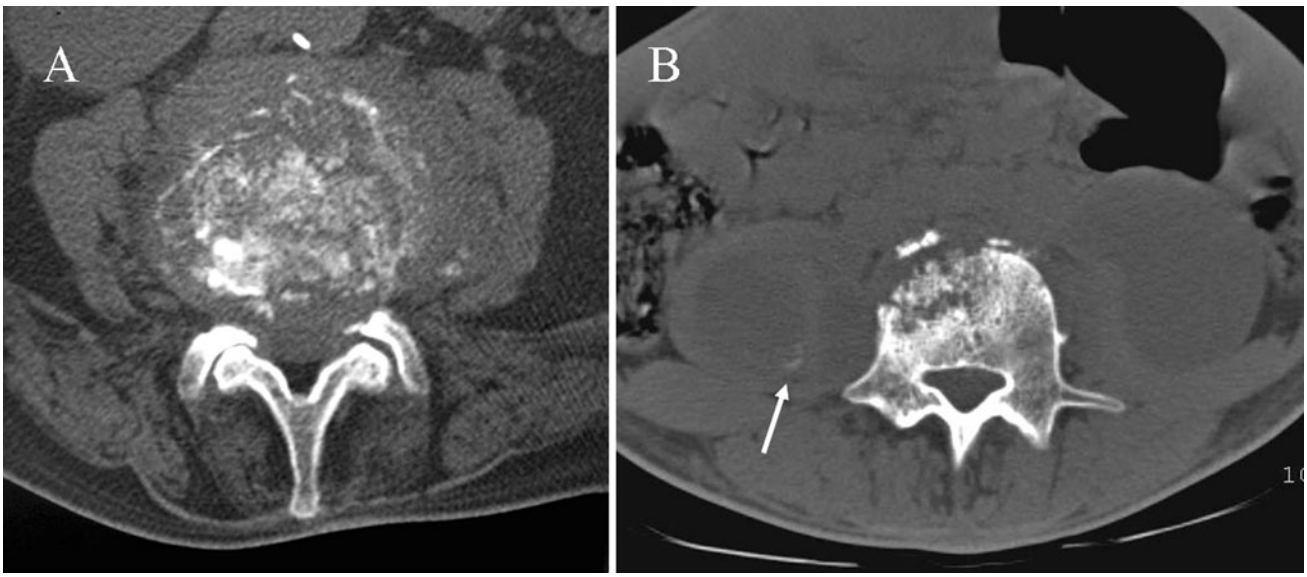

Fig. 2 Findings that suggest spinal TB. **a** Axial CT scan shows the fragmentary bone pattern. **b** Large paraspinal soft tissue abscesses with initial calcification of the wall (*arrow*)

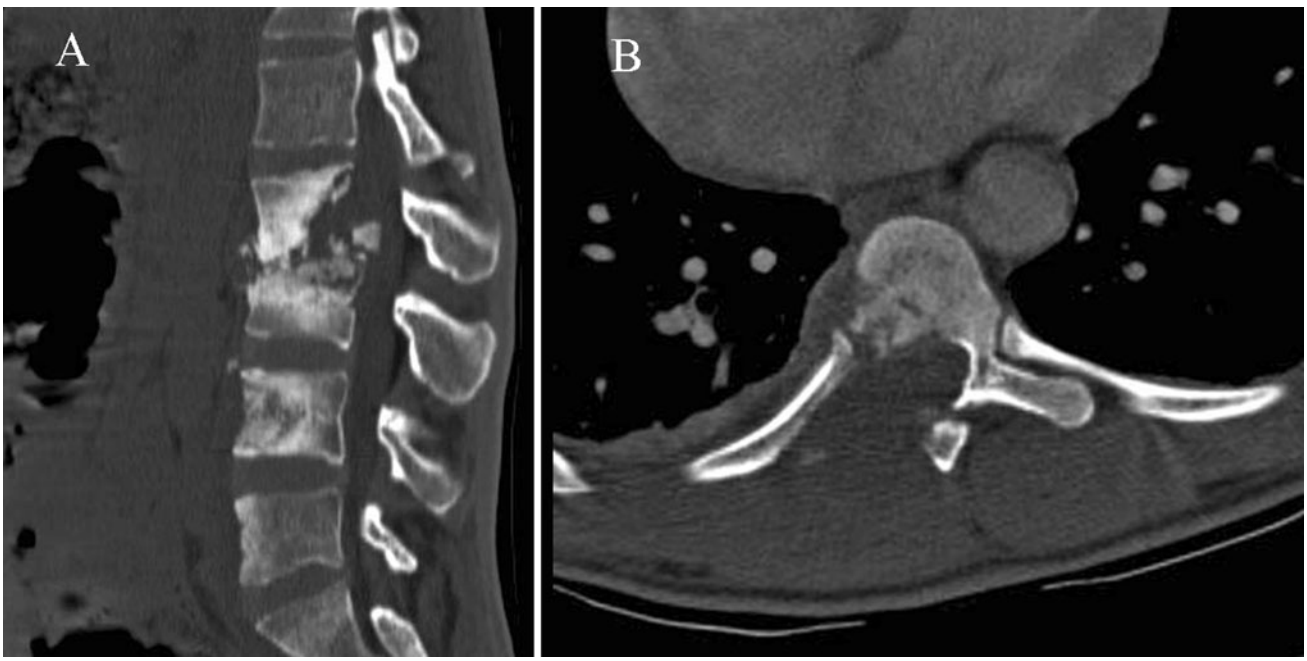

Fig. 3 Atypical radiographic findings. **a** Multilevel TB shows extensive bony sclerosis in four levels and intrasomatic infection disease of L4 without disk involvement. **b** Permeative osseous pattern involves costotransverse joint and adjacent soft tissues

[4–6, 22, 23, 25]. This is because radiographic changes are often present at the time of the initial study [5, 10, 11], as occurred in 70 % of our cases ($n = 21$). Furthermore, other entities can be excluded by X-rays. We recommend that oblique views must be included in X-ray series of spine to detect early changes involving anterolateral corners of the vertebra (Fig. 1).

The earliest findings are radiolucencies and the loss of definition of the plate margins [1, 4, 11, 14, 21, 24]. The most common appearance consists of vertebral body destruction (predominantly anterior), loss of disk height, erosion of end plates, vertebral geodes, bone sequestration, sclerosis and paravertebral masses [1, 2, 10, 13, 21, 23, 25] (Fig. 2). Calcification in paraspinal masses is highly suggestive of TB [1, 12, 21] (Fig. 2). However, the height of disk space can be preserved until the later stages of the infection [19] or be falsely preserved due to end-plate destruction [1, 20, 25]. The infection progresses to

dissemination into additional spinal segments resulting in the classic pattern of multilevel involvement. Advanced stages of the disease are characterized by: sclerosis from reparative processes, bony ankylosis, vertebral collapse and anterior wedging leading to progressive kyphosis and gibbus deformity [21, 24] (Fig. 3).

Atypical findings of spinal tuberculosis are increasingly observed and include: anterior subperiosteal lesion (aneurysmal syndrome), anterior vertebral scalloping with sparing of the disk, noncontiguous vertebral involvement, isolated involvement of the neural arch, central bony lesions without disk involvement, involvement of the craniovertebral junction, and reactive sclerosis resulting in an "ivory" vertebra [5, 10, 19, 21, 26, 27].

Regarding the radiological outcome, a considerable variability of radiological changes has been reported, that could occur in spite of a clinical response to medical treatment. Sclerosis, when present at early disease (50 % of patients) gives little information about clinical improvement although it is a feature of healing when the early disease is purely osteolytic. Bone destruction or loss of vertebral height progresses for up to 14 months, and recovery of vertebral body height is not seen earlier than 15 months after starting treatment. Changes in soft tissue masses, namely the progression of calcifiying debris, are useful for the follow-up. Ankylosis, which occurs in over 50 % of patients, is considered the surest evidence of healing [13].

In comparison with radiography, CT better evaluates radiographic findings and the lesion extent, due to its high contrast resolution and its tomographic nature. The new MDCT technology provides excellent multiplanar reconstruction imaging for the assessment of bone and soft tissue infection, essential for presurgical planning. Intravenous contrast administration clearly shows the multiloculated cystic paraspinal masses, enhancing the granulomatous tissue and the walls of abscesses located in both bone and soft tissues [5, 9]. Among the four types of body destruction described (fragmentary, osteolytic, subperiostal and localized), the fragmentary type predominates and consists of numerous residual bony fragments which frequently migrate into soft tissue masses. It is strongly suggestive of TB [3] (Fig. 2).

Paraspinal mass and abscess formation are found early in the disease, being reported in 45–100 % of spinal TB [3, 4, 14, 15, 23]. This lesion lies anterolateral to vertebral bodies and expands with tendency for distant spread along the tissue planes and epidural space (Fig. 3). An abscess rarely occurs in the absence of observable vertebral infection.

Secondary extension of TB into the posterior elements is not infrequent [3, 10] (Fig. 2). Isolated involvement of the vertebral arch or the extradural space is found in 2–10 % of cases [3, 26] being common in nonwhite patients and patients who have AIDS [16].

The advantages of CT over MRI are a more reliable detection of calcified foci and it also provides a guide to interventional procedures [1, 3, 9, 16, 17]. However, CT is inferior to MR imaging in the early assessment of the spinal canal disease [9, 16].

At the chronic stage some new radiological findings can be detected: involvement of the posterior elements, calcification of abscess wall, and fistulization to other distant structures resulting in new abscesses.

We reviewed 31 radiographic and 37 CT studies obtained from 48 patients diagnosed of spinal TB. Most of the diseases affected thoracic ($n = 15$) or lumbar segments ($n = 16$). Involvement of one spinal segment ($n = 15$) slightly predominates over multilevel disease ($n = 14$), the later essentially located in thoracic spine. On X-rays destructive pattern was found in 70 % ($n = 21$) of conventional images and multifragmentary pattern was founded in 81 % ($n = 30$) of CT studies. Soft tissue abscess was detected in 95 % of studies ($n = 35$) with calcification in 46 % ($n = 17$) and with epidural extension in 54 % ($n = 20$). As atypical findings we found the extension of the infection to costotransverse joint in 22 % ($n = 8$) of patients and the presence of intradiskal gas in one patient. Radiologic follow-up was possible in 21 patients of which 43 % ($n = 9$) clearly showed ankylosis.

Magnetic resonance imaging

MRI is considered the method of choice in spinal infection because it combines high sensitivity with satisfactory specificity [1, 2, 5, 9, 11, 28]. Signal changes occur early in the development of the disease, when no other image modality shows lesions. Short time inversion recovery (STIR) sequence detects initial infective focus as inflammatory edema [1]. However, MRI is not specific for infection [9, 20]. MRI is recommended when a spondylitis is suspected because early diagnosis avoids severe spinal or neurological complications. It enables anatomic localization of the disease in different planes, allows early detection of disk and bone destruction, and depicts extension in bone and soft tissues, and assesses skip lesions in noncontiguous spinal TB [6, 20]. Therefore, it is especially helpful in detecting the subclinical "spinal cord compression syndrome", in which the neuronal damage can be clearly seen [2]. Surgical election, choosing between anterior and posterior decompression, must be established on the basis of MRI [7]. New technological advances and compatible surgical materials now permit the performance of guided interventional proceedings [29].

Four different MRI patterns of disease are found in vertebral TB: paradiskal, anterior, central and posterior lesions. The majority of authors suggests that the onset of the spinal infection is paradiskal [17, 20].

Paradiskal infection begins in the vertebral metaphysis, eroding the cartilaginous end plate, leading to disk space narrowing due to the infection itself or to disk herniation into the end plate. Due to osseous resorption, end plate demineralization with loss of cortical bone is observed. Compared to pyogenic spondylitis, TB typically shows more sharply destructive margins with absence of reactive sclerosis.

The signal intensity decreases in the vertebral bodies on T1-weighted sequences, while signal increase in both T2-weighted imaging and STIR sequence. This is the result of the replacement of bone marrow by inflammatory exudates, cells and hyperhemia [25]. The infected disk appears as decreased space showing blurring of the bone limits. On T2-weighted sequences the low signal of intranuclear cleft dissapears and the disk exhibits a very-high signal. With gadolinium the infected disk enhancement is obvious, allowing differentiation of the non-affected part. But the non-enhanced disk image needs careful evaluation to avoid confusion with intradiskal abscess. On the other hand it must be noted that affected vertebral bodies can display non-enhancing image and be mistaken as normal [8].

The spreading of infection into the surrounding soft tissues is common, and usually progresses in anterolateral direction (Fig. 4). The invaded epidural fat and connective tissues often show a-low signal intensity on T1 images, and the STIR imaging facilitates visualization [25]. Abscessified collections often show high signal intensity on T1-weighted images with reduced signal intensity on T2-weighted sequences, as compared with cerebrospinal fluid signal. However, mixed signal intensity on both T1- and T2-weighted images can be observed in phlegmons as well as in fluid collections. In this case the use of gadolinium is particularly useful for differentiation [1, 25]. The abscess has a thin smooth wall contrast enhancement, whereas the phlegmon has uniform enhancement [30]. Between 55 and 96 % of paraspinal abscesses occur in the thoracic spine, they can spread through the ilio-psoas compartment and have the capacity to reach the retroperitoneum, pelvis or thigh [20] (Fig. 5). There is no relationship between the abscess size and the severity of the spondylodiskitis.

In the anterior pattern the infection starts in the corner of the vertebral body, it spreads to the adjacent vertebrae underneath the anterior longitudinal ligament (Fig. 4). Subligamentous dissemination stripes the periostium and the anterior longitudinal ligament from the vertebral surface. Periostium stripping makes the avascular vertebrae more vulnerable to infection. Combined ischemic and high pressure attacks produce scalloping of the anterolateral surface of the vertebral bodies ("gouge defect"). It may mimic bone tumor, metastatic lymph nodes or even an aorta aneurysm. Finally, the progression of bone lesion produces anterior vertebral collapse, leading to kyphosis ('hump'), typically seen in Pott's disease. MRI findings consist of a subligamentous abscess with contrast enhancement, preservation of the disks, and abnormal signal involving multiple vertebral segments with heterogeneous signal intensity (Fig. 6).

In central lesions the infection affects one single vertebral body. The disk remains healthy, since nutrition is provided from the adjacent vertebra. If the infection progresses, the whole vertebral body collapses, and can be confused with malignancy. Infection spreads to the contiguous vertebra or to the paraspinal space. MRI shows

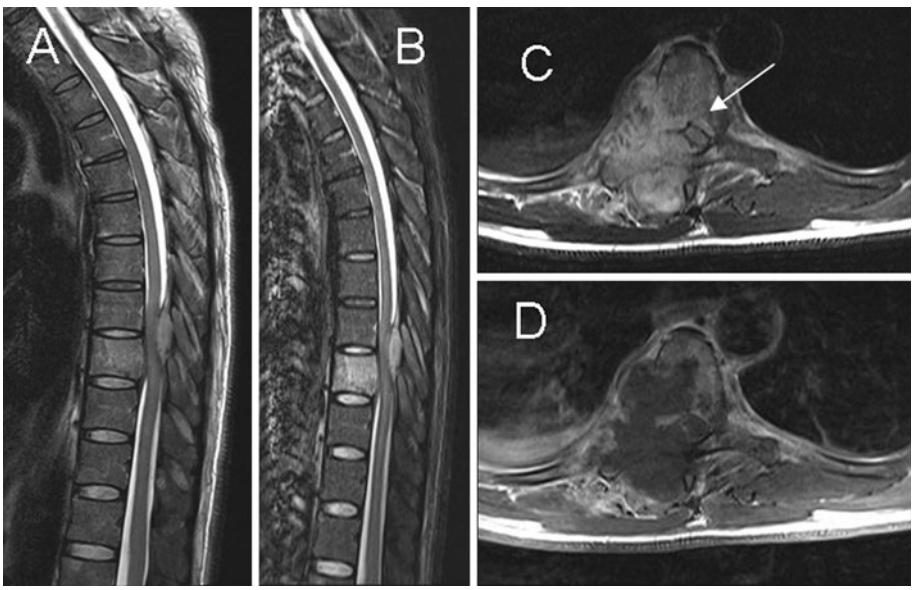

Fig. 4 Paradiskal pattern. **a**, **b** Sagittal T2-weighted imaging and STIR show hyperintense signal in the T9 vertebral body, suggesting bone marrow edema. **c**, **d** Axial T2- and T1-postcontrast weighted imaging show paradiskal involvement and infection spreading to the epidural space (*arrow*) with spinal cord compression

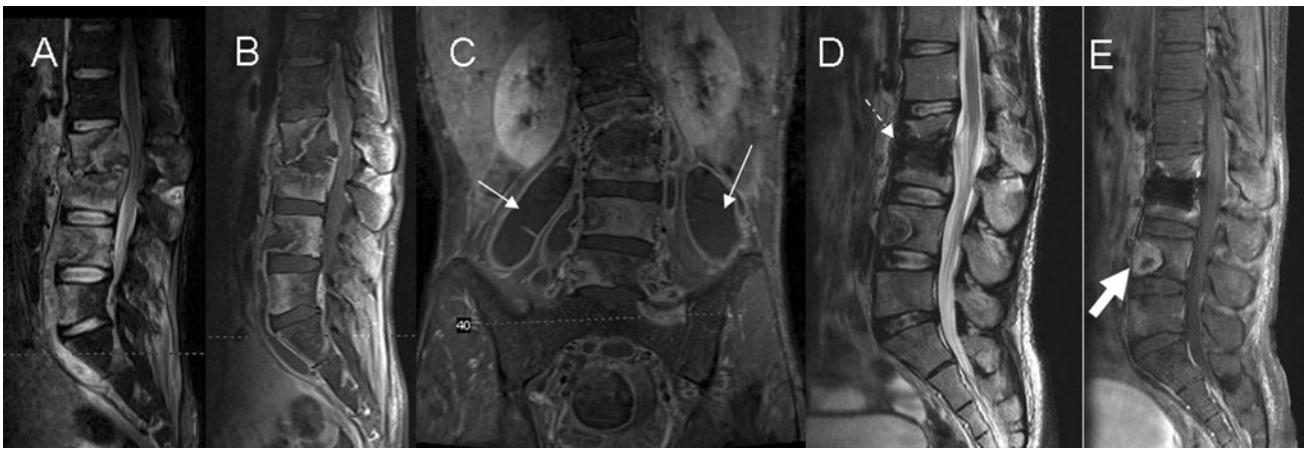

Fig. 5 Multisegmentary spread of disease with a large ilio-psoas abscess. **a**, **b** Sagittal STIR and T1-postcontrast weighted imaging show hyperintense signal and contrast enhancement involving multiple contiguous lumbar levels, Collapse of the bodies L2 and L3 in addition with spinal cord compression can be observed. **c** Coronal T1-postcontrast weighted imaging shows large bilateral soft tissue abscesses spreading along the ilio-psoas compartment (*arrows*). **d**, **e** Seven months after treatment MRI shows postoperative changes with bone graft (*dashed arrow*), improvement of the paravertebral abscess and decrease contrast enhancement in the soft tissues as compared to the study in acute disease

hypointense T1-weighted signal in a single vertebra and vertebral collapse with disk preservation (Fig. 7).

TB rarely affects the vertebral arch. The radiological pattern is frequently difficult to differentiate from metastasis, specially when disk space is preserved [12]. This occurs in only 5 % of cases [2] (Fig. 8).

There are not any definitive MRI findings to define spinal tuberculosis [11, 19–21] and biopsy is still be necessary [22]. However, many authors have attempted to find relevant differences between spinal tuberculosis and other disease entities, such as pyogenic infection or malignancies. Na-Young et al. [30] found that MRI showed a sensitivity of 100 %, a specificity of 80 % and an accuracy of 90 % in diagnosing TB when compared to pyogenic infection. Their most indicative signs of vertebral TB were: well-defined paraspinal abnormal signal, thin and smooth abscess wall, combination of both findings, presence of soft tissue or intraosseous abscess, subligamentous spread to three or more vertebral levels, involvement of multiple vertebral bodies, thoracic spine localization and hyperintense signal on T2-weighted images. No significant differences were obtained when the following were considered: involvement of intervertebral disk, disk space narrowing, epidural extension and contrast enhancement pattern.

In our study we evaluated 20 spinal MRI explorations. The paradiskal pattern was the most frequent and was observed in 80 % of cases ($n = 16$). Large abscesses affected paraspinal tissues in 65 % of patients ($n = 13$), vertebral body in 85 % ($n = 17$) and anterior epidural space in 80 % ($n = 16$). The infected bodies showed low T1 and hyperintense T2 signal in 95 % ($n = 19$) of cases. Heterogeneous gadolinium enhancement confirmed 80 % of studies ($n = 16$). Subligamentous spread was present in 40 % of multilevel infections ($n = 8$). Hyperintense T2 signal of the disk space was found in 85 % of cases ($n = 17$) and disk space narrowing in 60 % ($n = 12$). In later stages vertebral body destruction with collapse affected 70 % ($n = 14$) of cases and kyphotic deformity was found in 25 % ($n = 5$). Obvious spinal cord compression was detected in 65 % of studies ($n = 13$).

MRI follow-up was possible in only 45 % ($n = 9$) of all patients. The assessment of the success of medical treatment on the follow-up examinations is difficult. An early MRI imaging sign of healing is the decrease of contrast enhancement; this is expected a few weeks or months after beginning treatment. But it has limited value as it can persist in successfully treated cases [25], as occurred in 15 % ($n = 3$) of our patients. The resolution of process by means of MR imaging takes approximately 12 weeks [7, 8]. From 9 to 12 months after the treatment begins, the image shows increasing signal intensity on T1-weighted images where previous abnormalities were observed on T2 sequences as occurred in 50 % ($n = 10$) of our series (Figs. 5, 9). Therefore, T2 images revert to normal [7]. This can be due the stimulation of the fat conversion in the yellow bone marrow [12]. But sometimes on MRI performed in the course of a good response to treatment, the imaging findings may worsen showing more extensive disease and bone destruction during many months [2, 8].

Radionuclide studies

Nuclear medicine is a molecular imaging modality which can differentiate infectious from non-infectious disease, measure the metabolic rate of a lesion, detect multifocality

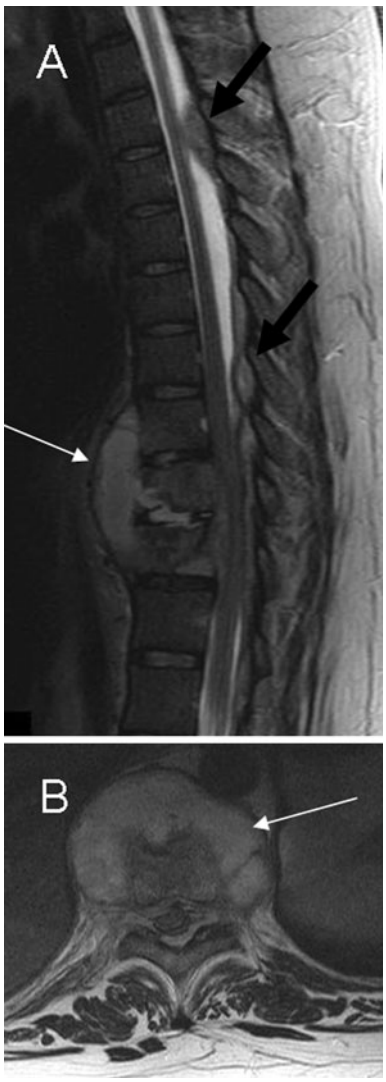

Fig. 6 **a**, **b** Sagittal and axial T2-weighted imaging show subligamentous infection involving three contiguous vertebral levels: T10–T12 with spondylodiskitis (*white arrow*) and large posterior epidural abscesses extending through epidural space to T5–T6 level (*black arrow*)

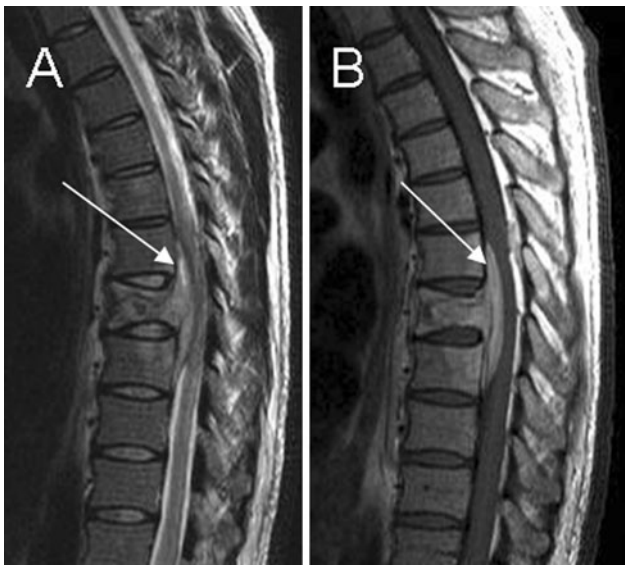

Fig. 7 Central pattern. **a**, **b** Sagittal T2 and T1-postcontrast weighted imaging show vertebral involvement and disk preservation. Note an anterior epidural abscess spreading to the adjacent vertebral bodies (*arrow*)

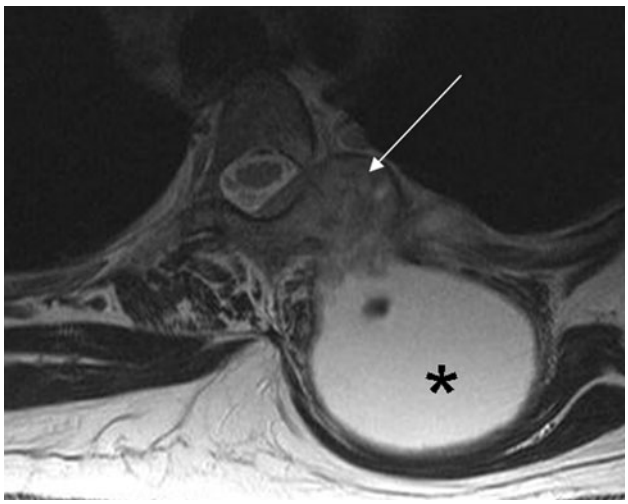

Fig. 8 Posterior pattern. Axial T2-weighted imaging shows a large cold abscess (*asterisk*) located in soft tissues and associated bone infection involving vertebral arch and costovertebral joint (*arrow*)

and also show the active disease which does not respond to treatment.

The most commonly used techniques in Pott's disease are bone scintigraphy with ^{99}mTc-Diphosphonates in combination with ^{67}Ga-citrate. Both sensitive but low specific, permit a whole-body evaluation. Their poor spatial resolution has been improved by means of SPET (single-photon emission tomography) and SPECT-CT for the exact localization of lesions. Another technique, ^{18}F-FDG PET–CT, is a positron-emission modality with higher spatial resolution, more sensitive and specific in diagnosing spondylitis. Nevertheless, neither of these techniques are able to disttinguish between pyogenic and non-pyogenic infection.

^{99}mTc-Diphosphonates is a bone tracer that identifies increased bone remodelling (active bone disease) [31, 32] with 75–95 % sensitivity [33, 34]. The three-phase bone scan evaluates the inflammatory process, therefore its sensitivity increases with intense infections but not in mild-to-moderate cases. Its diagnostic accuracy decreases when bone remodelling is associated with spondylitis, as when a fracture occurs. Increased contiguous vertebral activity will generally be observed, although disseminated TB and photopenic areas (related to an inadequate vascularization or bone destruction) can also be observed [32].

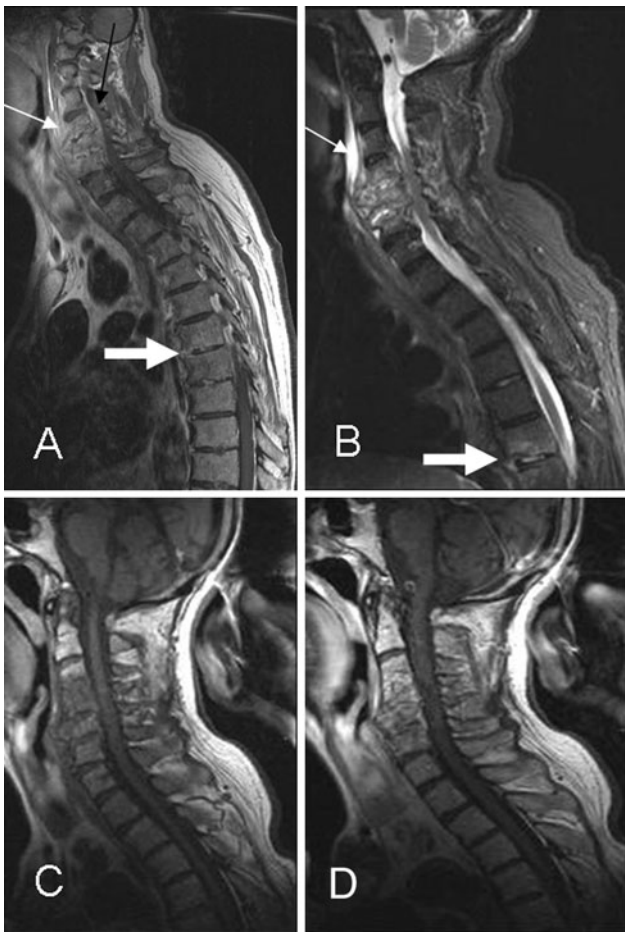

Fig. 9 Multisegmentary infection. **a**, **b** Sagittal T1-postcontrast weighted and STIR imaging show signs of advanced cervical infection with a large prevertebral abscess (*thin arrow*) and early skip lesion with epidural enhancement involving T6 and T7 levels (*thick arrow*). **c**, **d** Follow-up MRI 2 months later shows persistence of contrast enhancement in the cervical vertebral bodies with resolution of the prevertebral abscess

Gallium is an inflammatory-labelling isotope very helpful in the infection, unknown origin fever and chronic granulomatous diseases. Combined with Diphosphonates it can efficiently detect both osseous and soft tissue infection [32, 35, 36], with a sensitivity of 90 % and specificity of 78 %, [31, 37]. It has demonstrated its value in therapeutic response and also in the suspicion of a re-activation [35, 39]. Its positive interpretation is based on the coincidence of enhanced activity of both techniques in the same lesion or on a higher Gallium uptake where spatial discordance exists, e.g. when abscess is present.

PET–CT is another metabolic imaging technique, based on the glucose-cellular consumption, with a high-contrast rate between lesion and background [32, 35, 38] (Fig. 10). It is sensitive to chronic infections and specific in spondylitis [39], and it may differentiate infectious from non-infectious end-plate processes. Considering the low glucose consumption normally found in bone marrow and that the FDG uptake depends on the inflammatory/infectious activity, vertebral osteomyelitis can be easily detected, therefore a negative study will almost certainly exclude it. Compared to MRI, ^{18}F-FDG is not hampered by metallic artifacts [32]. Gratz [39] reported its superiority to MRI in detecting spondylitis, to Gallium in evaluating paraspinal abscesses, and to bone scan in differentiating advanced degenerative processes from infection. It may be useful in the follow-up, because FDG uptake normalization after treatment takes 3–4 months. Moreover, it has been proposed that relative uptake quantification (SUV) could distinguish between residual and non-residual lesions [35].

Interventional procedures

According to the principle "don't biopsy if not to be treated", percutaneous vertebral biopsy (PVB) is indicated when a lesion requires tissue sampling for determining diagnosis, stage of malignancy, and treatment. This occurs mainly in tumors and infections. Any vertebral segment can be biopsied by the percutaneous approach, although some difficulties can be found when C1 and C2 are involved.

Currently, CT is considered the best imaging-guide method for PVB as it provides the best results both in targeting lesions and the subsequent yield of diagnostic information [3, 17, 40–43]. Compared to open biopsy, closed biopsy has advantages including less morbidity, easy and quick execution, safety and absence of significant complications related to the procedure, precise location and, it is also cost effective [44–48]. Furthermore it has a positive influence in surgery planning and in the clinical outcome [49, 50].

Two types of samples must be obtained by PVB: the first by fine needle aspiration biopsy (FNAB), which contains either isolated cells or a block of cells without tissue structure and also contains material for microbiological culture if required; the second employs larger bore needles (17G to 8G) to obtain a core biopsy which maintains tissue structure allowing histological study and histological stage. Immunohistochemistry and genotypic analysis study can be practiced using both techniques.

Maximum benefit must be taken from any material obtained with regard to the diagnostic orientation and the type and quantity of the material. It must be broadly distributed between the different specialities, namely Pathology (which includes cytology and histology) and Microbiology. Before any broad differential diagnosis or if infection is suspected, material must be reserved for aerobic, anaerobic and mycobacteria culture. In addition, a cytology sample will help us to confirm the inflammatory

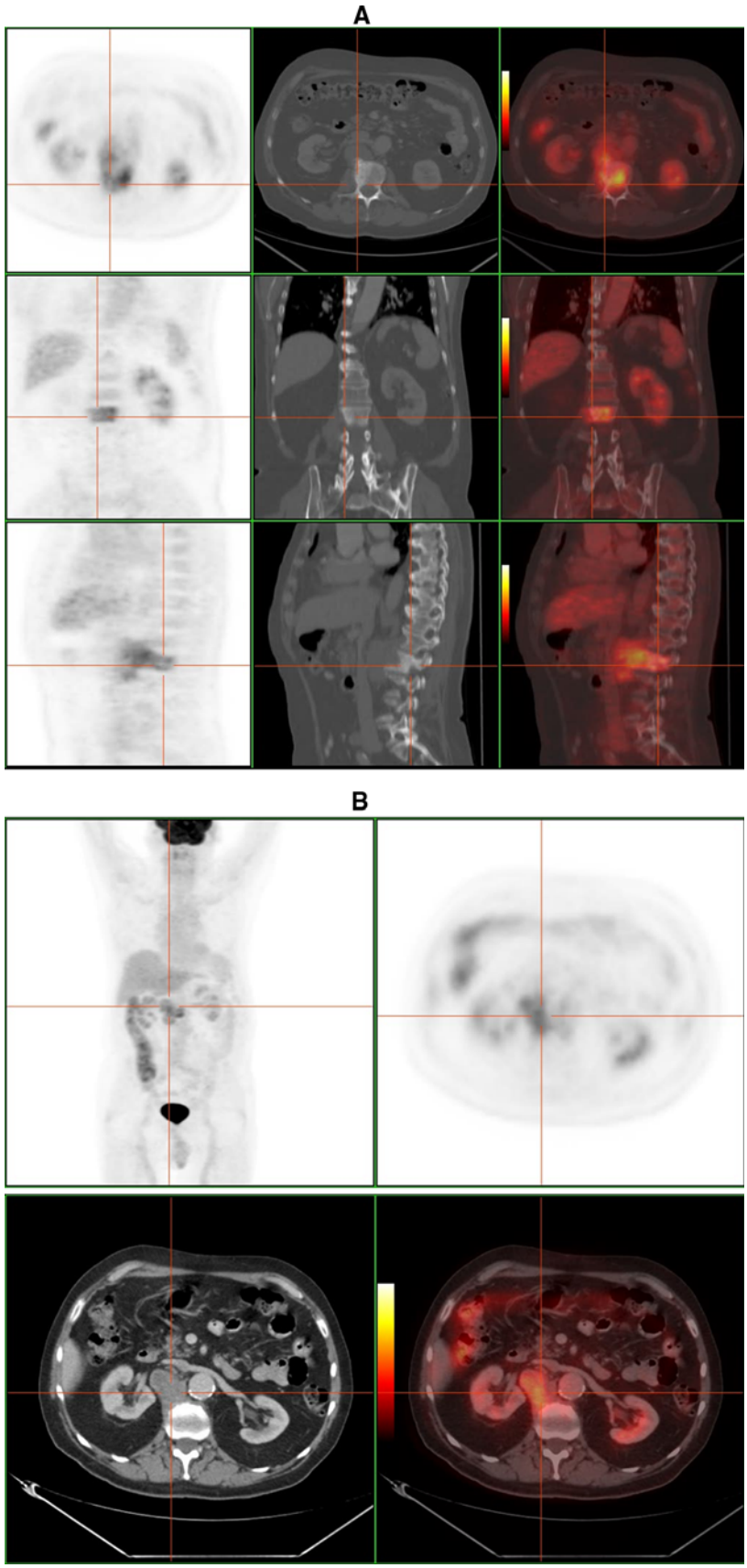

Fig. 10 F-18 FDG PET–CT study of a 50-year-old man with tuberculous spondylitis. **a** High FDG uptake located in L2 combined with bone sclerosis on CT scan. **b** There is a extraosseous fixation of the tracer, that corresponds to a paraspinal abscess according to CT image (courtesy of Dr. Lorenzo-Bosquet)

process (including direct visualization of pathogens in cases or fungi or mycobacteria infection), excluding other pathology. For these reasons we should always "cultivate the tumor and biopsy the infection".

In the case of spinal TB, PVB is indicated for the isolation of the microorganism (if no surgery is to be considered), when medical treatment is ineffective, when abscess drainage could be effective and finally if other entities, e.g. vertebral neoplasm, are being considered.

Conditions must be met before a PVB can be performed: (a) a multidisciplinary approach after an extensive clinical and radiological study; (b) information given to and consent received from the patient; (c) blood tests for coagulopathy; (d) a CT room under aseptic conditions. By using MDCT fluoroscopy mode, the technique requires prior location of the spinal level by scout view and the selection of best target area from the images obtained. At this stage the entry point, the lesion depth and the safest and shortest route to it are marked precisely. The samples are taken through a single puncture by using fine needles (22G) and thick bore-sized gaugues (17G to 8G) together coaxially (Fig. 11). The majority of PVB are performed through posterior access with the exception of those in lower cervical spine, which require an antero-lateral approach. For safety reasons, approach through bone structures (transpedicular, transcostovertebral, translaminar or transapophyseal) is preferred to approach through soft tissue. With regard to the lesion, it is more effective to biopsy lytic zones than blastic ones. Biopsy of paraspinal solid zones is preferred to biopsy of liquid collections (necrotic or cystic), however, aspiration is required when an abscess is present. When multiple lesions are present the biopsy site is determined according to safety of access and the aggressive image observations. A re-biopsy can be done if needed to confirm diagnosis, avoiding the area of the first biopsy or moving to another location if multiple lesions are present.

The procedure is usually performed under local anesthesia alone and in the outpatient form. With CT fluoroscopy near real-time imaging is possible, thus reducing the duration of procedure (average time 45 min) and improving the comfort of the patient. Aspiration material and core biopsy must be obtained in all cases. When spondylitis is suspected, PVB is performed by a single approach, but obtaining several representative samples placing needles into different parts of the lesion (paravertebral tissue and external disk area, central disk and bony end plates). When a soft tissue extension is observed a second puncture must be required to complete the procedure.

From May 1993 to June 2010, 720 patients underwent PVB of which 27 % ($n = 197$) resulted in spinal infection. Considering only the biopsy positive when proven culture or smear for acid-fast bacilli were obtained, the reported accuracy of CT-guided biopsy ranged from 61 to 93 % [4, 28, 41]. In our series the diagnosis of spinal TB was established at 78 % ($n = 29/37$), without any significant complication. Therefore, we conclude that CT-guided PVB is an adequate and accurate method in the diagnosis of Pott's disease.

Percutaneous drainage of abscesses is a safe and effective alternative to open surgical treatment and is indicated

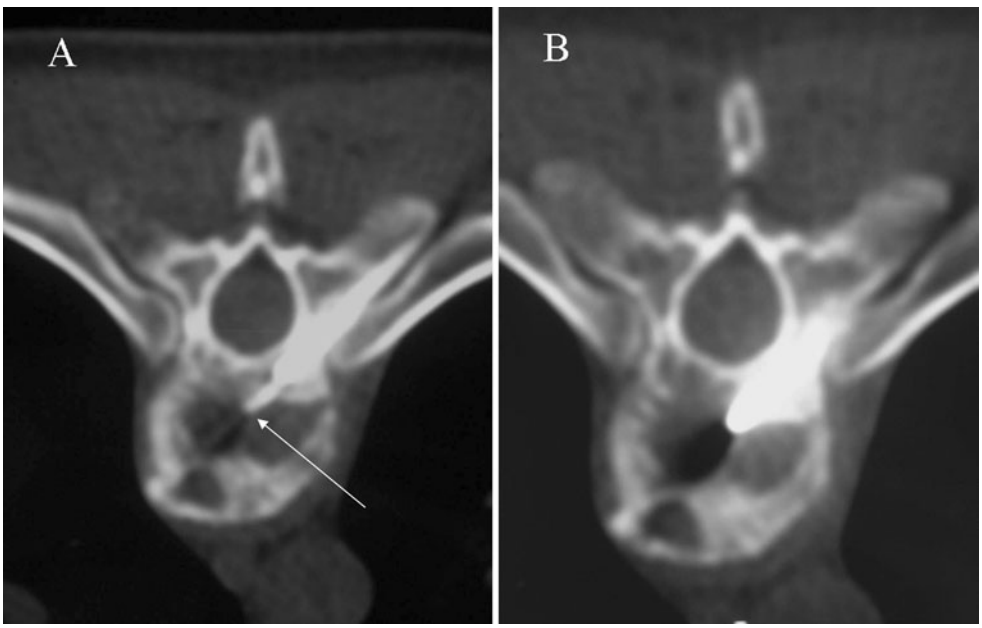

Fig. 11 CT fluoroscopy images show the coaxial percutaneous CT-guided technique for spinal biopsy. **a** Initial advance of fine needle through large needle for aspiration biopsy (*arrow*). **b** Next step which consists of directing the large needle into the disk and end plates, to obtain samples of core biopsy

when neurological pressure symptoms or a lack of response to medical treatment occur [51]. It can also be beneficial in completing medical treatment of large iliopsoas abscesses [5, 17].

Conclusion

Pott's disease is a common cause of spondylodiskitis. It requires early diagnosis for successful therapy to prevent severe morbidity. Imaging studies, namely MRI and CT, are important tools for: characterizing the lesion, performing biopsy, planning surgery, evaluating the success of treatment and detecting complications in the follow-up.

Conflict of interest None.

References

1. Jevtic V (2004) Vertebral infection. Eur Radiol 14:E43–E52
2. Cormican L, Hammal R, Messenger J, Milburn HJ (2006) Current difficulties in the diagnosis and management of spinal tuberculosis. Postgrad Med J 82:46–51
3. Jain R, Sawhney S, Berry M (1993) Computed tomography of vertebral tuberculosis: patterns of bone destruction. Clin Radiol 47:196–199
4. Lindahl S, Nyman RS, Brismar J, Hugosson C, Lundstedt C (1996) Imaging of tuberculosis. IV. Spinal manifestations in 63 patients. Acta Radiol 37:506–511
5. Moore SL, Rafii M (2001) Imaging of musculoskeletal and spinal tuberculosis. Radiol Clin North Am 39(2):329–342
6. Polley P, Dunn R (2009) Noncontiguous spinal tuberculosis: incidence and management. Eur Spine J 18:1096–1101
7. Sharif HS, Clarck DC, Aabed MY, Haddad MC, Al-Deeb SM, Yakub B, Al-Moutaery KR (1990) Granulomatous spinal infections: MR imaging. Radiology 177:101–107
8. Tins BJ, Di PL, Cassar-Pullicino VN (2004) MR imaging of spinal infection. Semin Musculoskelet Radiol 8(3):215–229
9. De Vuyst D, Vanhoenacker F, Gielen J, Bernaerts A, De Schepper AM (2003) Imaging features of musculoskeletal tuberculosis. Eur Radiol 13:1809–1819
10. Ousehal A, Gharbi A, Zamiati W, Saidi A, Kadiri R (2002) Imagerie di Mal de Pott. Neurochirurgie 48(5):409–418
11. Danchaivijitr N, Temram S, Thepmonggkhol K, Chiewvit M (2007) Diagnostic accuracy of MR imaging in tuberculous spondylitis. J Med Assoc Thai 90(8):1581–1589
12. Smith A, Weinstein MA, Mizuschima A, Coughin B, Hayden SP, Lakin MM, Lanzieri CF (1989) MR imaging characteristics of tuberculous spondylitis vs vertebral osteomyelitis. AJR 153:399–405
13. Boxer DI, Pratt C, Hine AL, McNicol M (1992) Radiological features during and following treatment of spinal tuberculosis. Br J Radiol 65:476–479
14. Harisinghani M, McLoud T, Shepard JA, Ko J, Shroff M, Mueller P (2000) Tuberculosis from head to toe. Radiographics 20:449–470
15. Yusof MI, Hassan E, Rahmat N, Yunus R (2009) Spinal tuberculosis. Spine 34(7):713–717
16. Shanley DJ (1995) Tuberculosis of the spine: imaging features. AJR 164:659–664
17. Dinç H, Ahmetoglu A, Baykal S, Sari A, Sayil Ö, Gümele HR (2002) Image-guided percutaneous drainage of tuberculous iliopsoas and spondilodiskitic abscesses: midterm results. Radiology 225:353–358
18. Messenger HJ, Milburn HJ (2006) Current difficulties in the diagnosis and management of spinal tuberculosis. Postgrad Med 82:46–51
19. Desai SS (1994) Early diagnosis of spinal tuberculosis by MRI. J Bone Joint Surg 76B(6):863–869
20. Moorthy S, Prabhu N (2002) Spectrum of MR imaging findings in spinal tuberculosis. AJR 179:979–983
21. Tali ET (2004) Spinal infections. Eur J Radiol 50:120–123
22. Hatem SF, Schils JP (2000) Imaging of infections and inflammatory conditions of the spine. Semin Musculoskelet Radiol 4(3):329–347
23. LaBerge JM, Brant-Zawadzki M (1984) Evaluation of Pott's disease with computed tomography. Neuroradiol 26:429–434
24. Burrill J, Williams C, Bains G, Conder G, Hine A, Misra R (2007) Tuberculosis: a radiologic review. Radiographics 27:1255–1273
25. Forrester DM (2004) Infectious spondylitis. Semin Ultrasound CT MRI 25:461–473
26. Babhulkar SS, Tayade WB, Babhulkar SK (1984) Atypical spinal tuberculosis. J Bone Joint Surg (Br) 66-B(2):294–296
27. Yalniz E, Pekindil G, Aktas S (2000) Atypical tuberculosis of the spine. Yonsei Med J 41(5):657–661
28. Jain AK (2010) Tuberculosis of the spine. A fresh look at an old disease. J Bone Joint Surg (Br) 92B:905–913
29. Blanco R, Ojala R, Kariniemi J, Niinimaki J, Tervonen O (2005) Interventional and intraoperative MRI at low field scanner, a review. Eur J Radiol 56:130–142
30. Jung NY, Jee WH, Ha KY, Park CK, Byun JY (2004) Discrimination of tuberculous spondylitis from pyogenic spondylitis on MRI. AJR 182:1405–1410
31. Lin WY, Wang SJ, Cheng KY, Shen YY, Changlai SP (1998) Diagnostic value of bone and Ga-67 imaging in skeletal tuberculosis. Clin Nucl Med 23(11):743–746
32. Gemmel F, Rijk PC, Collins JMP, Parlevliet T, Stumpe KD, Palestro CJ (2010) Expanding role of 18F-fluoro-D-deoxyglucose PET and PET/CT in spinal infections. Eur Spine J 19:540–541
33. Pandit HG, Sonsale PD, Shikare SS, Bhojraj SY (1999) Bone scintigraphy in tuberculous spndylodiscitis. Eur Spine J 8(3):205–209
34. Palestro CJ, Kim CK, Swyer AJ, Vallabhajosula S, Goldsmith SJ (1991) Radionuclide diagnosis of vertebral osteomyelitis: indium 111-leukocyte and technetium-99 m-methylene diphosphonate bone scintigraphy. J Nucl Med 32:1861–1865
35. Kim SJ, Kim IJ, Suh KT, Kim YK, Lee JS (2009) Prediction of residual disease of spine infection using F-18 FDG PET/CT. Spine 34:2424–2430
36. Gratz S, Dörner J, Oestmann JW, Opitz M, Behr T, Meller J, Grabbe E, Becker W (2000) 67-Ga citrate and 99Tc-MDP for estimating the severity of vertebral osteomyelitis. Nucl Med Commun 21:111–120
37. Lisbona R, Derbekyan V, Novales-Diaz J, Veksler A (1993) Gallium 67 scintigraphy in tuberculous and non-tuberculous infectious spondylitis. J Nucl Med 34(5):853–859
38. Schmitz A, Kälicke T, Willkomm P, Grünwald F, Kandyba JJ, Schmitt O (2000) Use of fluorine-18 fluoro-2-deoxy-D-glucose positron emission tomography in assessing de process of tuberculous spondylitis. J Spinal Disord 13(6):541–544
39. Gratz S, Dorner J, Fischer U, Behr TM, Behe M, Altenvoerde G, Meller J, Grabbe E, Becker W (2002) F-18-FDG hybrid PET in patients with suspected spondylitis. Eur J Nucl Med Mol Imaging 29:516–524
40. Michel SC, Pfirrmann CWA, Boos N, Hodler J (2006) CT-guided core biopsy of subchondral bone and intervertebral space in suspected spondilodiskitis. AJR 186:977–980

41. Dupuy DE, Rosenberg AE, Punyaratabandhu T, Hong Tan M, Mankin H (1998) Accuracy of CT-guided needle biopsy of musculoskeletal neoplasms. AJR 171:759–762
42. Anwar Hau M, Kim JI, Kattapuram S, Hornicek FJ, Rosenberg AE, Gebhardt MC, Mankin HJ (2002) Skeletal Radiol 31:349–353
43. Peh WCG (2006) CT-guided percutaneous biopsy of spinal lesions. Biomed Imaging Interv J 2(3):e25
44. Springfield DS, Rosenberg A (1996) Biopsy: complicated and risky. J Bone Joint Surg 78A:639–643
45. Bellaïche L, Hamze B, Parlier-Cau C, Laredo JD (1997) Percutaneous biopsy of musculoskeletal lesions. Semin Musculoskeletal Radiol 1:177–187
46. Heare TC, Enneking WF, Heare MJ (1989) Staging techniques and biopsy of bone tumors. Orthop Clin North Am 20:273–285
47. Fraser-Hill MA, Renfrew DL, Hilsenrath PE (1992) Percutaneous needle biopsy of musculoskeleta lesions. 2. Cost-effectiveness. AJR 158:813–817
48. Skrzynsky MC, Biermann JS, Montag A, Simon MA (1996) Diagnostic accuracy and charge-savings of outpatient core needle biopsy compared with open biopsy of musculoskeletal tumors. J Bone Joint Surg 78A:644–649
49. Jelinek JS, Murphey MD, Welker JA, Hensaw RM, Kransdorf MJ, Shmookler BM, Malawer MM (2002) Diagnosis of primary bone tumors with image-guided percutaneous biopsy: experience with 110 tumors. Radiology 223:731–737
50. Ward WG, Kilpatrick S (2000) Fine needle aspiration biopsy of primary bone tumors. Clin Orthop 373:60–87
51. Nigam V, Chhabra HS (2007) Easy drainage of presacral abscess. Eur Spine J 16:S322–S325